Phase-object analysis with a speckle interferometer

Luciano Angel

Departamento de Ciencias Básicas, Universidad Escuela de Administración, Finanzas y Tecnología, Medellín, Colombia

Myrian Tebaldi, Marcelo Trivi, and Nestor Bolognini

Centro de Investigaciones Ópticas (Consejo Nacional de Investigaciones Científicas y Técnicas-CIC) and Unidad de Investgación y Desarollo OPTIMO (Facultad Ingneniená, Universidad Nacional de La Plata), La Plata 1900, Argentina

Received October 31, 2001

We describe the characteristics of a double-exposure specklegram obtained through a double-aperture system, by introduction of a wedge in front of one aperture in one exposure. It is assumed that a uniform displacement of the diffuser is produced between exposures. The average intensity distribution and visibility of the interferometric fringes in the Fourier plane are analyzed. An alternative interferometric technique for phase-object detection is proposed. © 2002 Optical Society of America

OCIS codes: 120.6160, 120.5050.

Several techniques for image processing and metrology by introduction of frequency carriers into a random diffuser have been implemented. Some of these proposed techniques are based on internal modulation of speckles, which can be achieved by location of a mask with two or more apertures in front of the imaging lens.[1,2] In some applications the number of apertures or the aperture shape of the optical system is modified between exposures.[3,4] Also, the use of several multiaperture shearing interferometers has been proposed.[5] In those arrangements the pupil of the optical system does not change between exposures. In Ref. 2, a method for image subtracting was reported that uses a uniform plate to control the phase of the wave passing through one of the apertures in a double-aperture system.

In this Letter we analyze the properties of a double-exposed specklegram generated through a double-aperture system by assuming that a wedge is located front of one of the apertures in one exposure. A comparison between theoretical simulations and experimental results is presented by consideration of a parallel plate and a wedge.

The setup for recording is schematized in Fig. 1(a). The diffuser, R, is illuminated by a laser beam of wavelength λ_W and imaged in the $x-y$ plane by lens L_1. Z_0 and Z_C are the distances from the diffuser to the lens and from the lens to the image plane, respectively. A pupil mask with two identical apertures is located in front of the lens. In the second exposure a wedge is introduced in front of one of the pupil apertures. Furthermore, an in-plane displacement of the diffuser is introduced between exposures. This displacement is necessary to generate correlation fringes in the Fourier plane.

The loci of the apertures are given by

$$a_j(u,v) = a(u-u_j, v-v_j) = \begin{cases} 1 & \text{inside the } j\text{th aperture} \\ 0 & \text{otherwise} \end{cases}, \quad j = 1,2,$$

where the vectors (u_1, v_1) and (u_2, v_2) represent the aperture centers. The function $a(u,v)$ describes the aperture shape, and $d = [(u_2-u_1)^2 + (v_2-v_1)^2]^{1/2}$ defines the distance between the aperture centers. On this basis, the pupils employed are given by $P^1(u,v) = a(u-u_1, v-v_1) + a(u-u_2, v-v_2)$ and $P^2(u,v) = a(u-u_1, v-v_1) + t\exp[i(\gamma+\tau u)]a(u=u_2, v=v_2)$, where t and $\gamma + \tau u$ represent the real amplitude transmission and the linear phase shift introduced by the wedge, respectively. We consider the u axis to be perpendicular to the thin edge of the wedge.

Analysis of the specklegram is carried out with the arrangement depicted in Fig. 1(b). The specklegram is illuminated with an expanded laser beam of wavelength λ_R, and the transmitted light is Fourier transformed through lens L_2 of focal length f. If a pupil with square apertures of side D is utilized, then the average intensity in the Fourier plane (U, V) results:

$$\langle I(U,V)\rangle = \langle I^0(U,V)\rangle + \langle I^{+1}(U,V)\rangle + \langle I^{-1}(U,V)\rangle, \tag{1}$$

where

$$\langle I^0(U,V)\rangle = KD^2 \operatorname{trian}\left(\frac{\vartheta U}{D}\right)\operatorname{trian}\left(\frac{\vartheta V}{D}\right) \times \{3 + t^4 + 2[1 + t^4 + 2t^2\cos(\vartheta\tau U)]^{1/2} \times \cos\left[\frac{2\pi}{\lambda_R f}(U\Delta X^{12} + V\Delta Y^{12}) - \Phi(U)\right]\}, \tag{2}$$

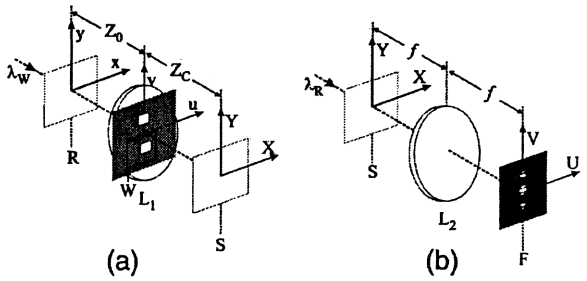

Fig. 1. Experimental setup: S's, specklegram image planes; F, Fourier plane; L_1 and L_2, lenses. See text for other definitions.

0146-9592/02/070506-03$15.00/0

$$\langle I^{\pm 1}(U,V)\rangle = KD^2 \,\mathrm{trian}\left(\frac{\vartheta U \mp u_{12}}{D}\right)\mathrm{trian}\left(\frac{\vartheta V \mp v_{12}}{D}\right) \times \left(1 + t^2 + 2t\,\mathrm{sinc}\left\{\frac{\tau D}{2\pi}\left[1 - \frac{\vartheta U \mp u_{12}}{D} \times \mathrm{sign}(\vartheta U \mp u_{12})\right]\right\}\cos\left\{\frac{2\pi}{\lambda_R f}\left[U\left(\Delta X^{12} - \frac{\lambda_W Z_C}{4\pi}\tau\right) + V\Delta Y^{12}\right] \mp \gamma \mp \frac{u_1 + u_2}{2}\tau\right\}\right), \quad (3)$$

where $\langle I^0(U,V)\rangle$, $\langle I^{+1}(U,V)\rangle$, and $\langle I^{-1}(U,V)\rangle$ are the average intensity distributions corresponding to the zero and the (+1) and (−1) diffracted orders, respectively, and K is a constant. The vector $(u_{12}, v_{12}) = (u_2 - u_1, v_2 - v_1)$ represents the relative position of the apertures, $(\Delta X^{12}, \Delta Y^{12})$ is the relative displacement between the diffuser images and $\vartheta = \lambda_W Z_C/\lambda_R f$. Note that $(\Delta X^{12}, \Delta Y^{12}) = -(Z_C/Z_0)(\Delta x^{12}, \Delta y^{12})$, where $(\Delta x^{12}, \Delta y^{12})$ is the diffuser displacement. Furthermore, the phase term $\Phi(U) = -\tan^{-1}[t^2 \sin(\vartheta\tau U)]/[1 + t^2\cos(\vartheta\tau U)]$ is introduced in Eq. (2).

From Eqs. (2) and (3) it follows that the fringe visibility for the zero and diffracted orders are

$$\mathbf{V}^0(U) = \frac{2}{3 + \tau^4}[1 + t^4 + 2t^2\cos(\vartheta\tau U)]^{1/2}, \quad (4a)$$

$$\mathbf{V}^{\pm 1}(U) = \frac{2t}{1 + t^2}\left|\mathrm{sinc}\left\{\frac{D\tau}{2\pi}\left[1 - \frac{\vartheta U \mp t_{12}}{D} \times \mathrm{sign}(\vartheta U \mp u_{12})\right]\right\}\right|. \quad (4b)$$

Let us consider a specklegram obtained through a parallel plate located in front of one aperture in the second exposure. Here the dihedral angle of the wedge is null, i.e., $\tau = 0$. In this case, in Eqs. (2) and (3) we must have $\tau = 0$ and $\gamma \neq 0$. The cosine terms in Eqs. (2) and (3) stand for the interferometric fringes observed in the diffracted orders. The presence of factor γ in the cosine function of Eq. (3), which corresponds to the lateral orders, modifies the interferometric-fringe modulation. Note that the amount γ determines the interferometric-fringe shifting in the Fourier plane. The minus sign in Eq. (3) is applied to the (+1) order and the plus sign to the (−1) order. Then, the fringe is shifted in opposite directions in the (+1) and (−1) orders. The interferometric fringes experience a global shift, which is produced in opposite directions in the lateral orders, while the zero order is not affected.

Furthermore, when a parallel plate ($t_2 \equiv t$) is introduced in the second exposure, the visibility of the fringes is determined only by the transmission of the plate employed.

Let us compare the theoretical average intensity distribution in the Fourier plane obtained by use of Eqs. (2) and (3) with the experimental results. The setup shown in Fig. 1 is employed and the parameters are $t = -0.8$, $\gamma = \pi$, $\lambda_R = 633$ nm, $\lambda_W = 514$ nm, $D = 3.8$ mm, $Z_C = 485$ mm, $d = 10$ mm, $f = 100$ mm, $\Delta X^{12} = 0$, and $\Delta Y^{12} = 142 \times 10^{-3}$ mm. The displacement, ΔX^{12} and ΔY^{12}, was done with a precision translation stage within 1-μm accuracy. Note that the centers of the pupils belong to the v axis. See also the coordinate axis attached to the results.

The results of Figs. 2(a) and 2(b) were experimentally obtained by use of a conventional recording scheme without and with a parallel plate in front of one of the pupil apertures in the second exposure, respectively. These experimental results can be compared with the theoretical simulations of Figs. 2(c) and 2(d), obtained by use of Eqs. (2) and (3), corresponding to the average intensity of the zero and the lateral orders. The same parameters are employed as in the experimental case. There is apparent agreement between results.

Let us analyze the interferometric fringes that result when a wedge whose dihedral angle is not null ($\gamma \neq 0$ and $\tau \neq 0$) is used in the second exposure. When the diffuser displacement and the thin edge of the wedge are parallel, Eq. (3) predicts that the fringes will tilt. This fringe rotation is accompanied by increasing spatial frequency. This phenomenon is confirmed by the results shown in Fig. 3. The magnitude of this rotation increases as the τ value increases. Note that if the wedge is introduced in the first exposure rotation in the opposite direction is produced. The angle between the fringes and the U axis is given by $\alpha = \tan^{-1}(\lambda_W Z_C \tau/4\pi\Delta Y^{12})$.

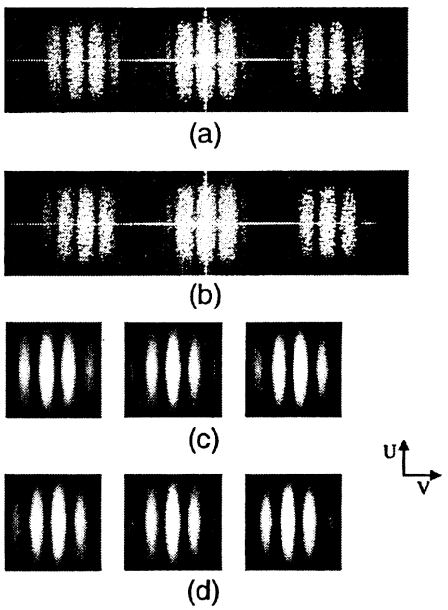

Fig. 2. Experimental results (a) without and (b) with a parallel plate in front of one aperture in the second exposure and (c) and (d) the corresponding theoretical simulations. The center images in (c) and (d) represent the zero order, and the left and right images represent the (−1) and (+1) orders, respectively.

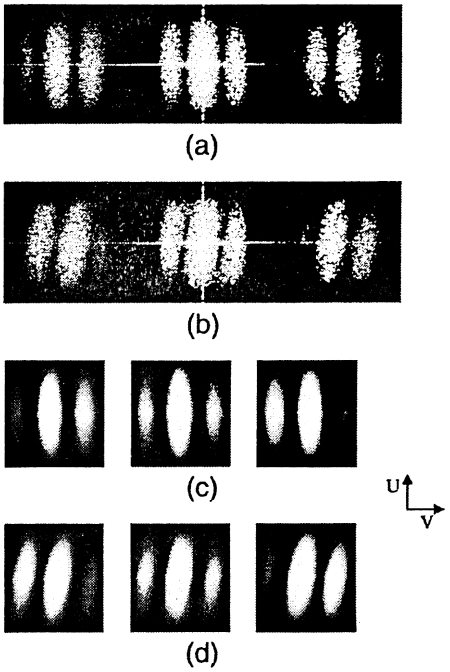

Fig. 3. Experimental results (a) without and (b) with a wedge in front of one aperture in the second exposure and (c) and (d) the corresponding theoretical simulations. The thin edge wedge and the diffuser displacement are parallel. The central images in (c) and (d) represent the zero order, and the left and right images represent the (−1) and (+1) orders, respectively.

Another phenomenon is the appearance of an amplitude modulation of the fringes that diminishes its visibility: This fact is described by the term $2t\ \mathrm{sinc}((\tau D/2\pi)\{1 - [(\vartheta U \mp u_{12})/D]\mathrm{sign}(\vartheta U \mp u_{12})\})$ in Eq. (3). As far as τ increases, visibility in the diffracted-order centers decreases. When the magnitude of τ increases further, the visibility decreases until a null value is reached along one or several lines running parallel to the edge of the wedge. It should be pointed out that the fringe visibility decreases as τ and the angle α increase. The interferometric-fringe visibility at the central point of each diffracted order is $\mathbf{V}^{\pm 1}(\mp d') = (2t)/(1 + t^2)|\mathrm{sinc}(D\tau/2\pi)|$. As a consequence, the visibility drops to zero at the center of the diffracted order, provided that $\tau D = m2\pi$, for $m = \pm 1, \pm 2, \ldots$. To prevent the visibility of the diffracted orders from decreasing below a certain value, we must impose the condition that the magnitude of τ does not exceed a limit defined in terms of the remaining experimental parameters. For example, for a minimum visibility higher than $-t/(1 + t^2)$, it must hold that $D|\tau|/2\pi < 0.6$. In our case, $D = 3.8$ mm, then $|\tau| < 992\ \mathrm{m}^{-1}$. Note that the wedge dihedral angle is $\beta = \tan^{-1}[\tau\lambda_W/(n - 1)2\pi]$, where n is the refractive index of the wedge. Then, if $n = 1.5$ and $\lambda_W = 514$ nm and $|\tau| < 992\ \mathrm{m}^{-1}$, dihedral angle β must be less than 33.5 arcsec.

In Fig. 3 we show the average intensity distribution in the Fourier plane obtained by introduction of a wedge in the second exposure ($\gamma = 0.6$ and $\tau = 750\ \mathrm{m}^{-1}$) so that the thin edge wedge and the diffuser displacement are parallel. The results of Figs. 3(a) and 3(b) are obtained without and with introduction of a wedge in front of one aperture in the second exposure by a conventional recording scheme, respectively. The parameters employed are $t = 0.8$, $\gamma = 0.6$, $\tau = 750\ \mathrm{m}^{-1}$, $\lambda_R = 633$ nm, $\lambda_W = 514$ nm, $D = 3.8$ mm, $Z_C = 485$ mm, $d = 10$ mm, $f = 100$ mm, $\Delta X^{12} = 0$, and $\Delta Y^{12} = 94 \times 10^{-3}$ mm. These experimental results can be compared with the theoretical simulations [Figs. 3(c) and 3(d)] corresponding to the average intensity of the zero and the lateral orders obtained by use of Eqs. (2) and (3) and the same parameters as in the experimental case. With the parameters of Fig. 3, the resulting angle α is 9°.

In our method the phase object is characterized as changes of correlation fringes. To this purpose, the average intensity and visibility of these fringes in the Fourier plane were evaluated. We discussed the phenomena observed in the diffracted orders and compared the results with those obtained with a conventional double-exposed specklegram. The changes in the interferometric fringes can also be evaluated in terms of the parameters that define the phase object employed in each experiment. It should be pointed out that this method can be performed in real time by use of a photorefractive crystal as a recording medium.[4]

This interferometer is well suited to measurement of very small angles concerning phase objects. For instance, the time-varying thickness map of vertical soap films could be analyzed.[6] This study gives information on the nature and range of the intermolecular forces that are responsible for the film formation. This experiment is implemented by storage of a reference speckle image in a buffer memory. Afterward, the evolution of the film can be displayed by real-time addition of the successive status of the speckle pattern and the reference image. By application of a real-time fast Fourier-transform algorithm to the resulting pattern, the correlation fringes are obtained and the film formation can be monitored.

M. Tebaldi's e-mail address is myrian@odin.ciop.unlp.edu.ar.

References

1. D. Duffy, Appl. Opt. **11,** 1778 (1972).
2. H. Rabal, N. Bolognini, E. Sicre, and M. Garavaglia, Opt. Commun. **34,** 7 (1980).
3. M. Tebaldi, L. Angel, M. Trivi, and N. Bolognini, Opt. Commun. **168,** 55 (1999).
4. L. Angel, M. Tebaldi, N. Bolognini, and M. Trivi, J. Opt. Soc. Am. A **17,** 107 (2000).
5. R. Mohanty, C. Joenathan, and R. Sirohi, Appl. Opt. **24,** 3106 (1985).
6. V. Greco and G. Molesini, Sci. Technol. **7,** 96 (1996).